Structural Studies of the Roles of Residues 82 and 85 at the Interactive Face of Cytochrome *c*[†,‡]

Terence P. Lo, J. Guy Guillemette,[||] Gordon V. Louie,[§] Michael Smith, and Gary D. Brayer*

Department of Biochemistry, University of British Columbia, Vancouver, British Columbia, Canada V6T 1Z3

Received August 24, 1994; Revised Manuscript Received October 3, 1994[⊗]

ABSTRACT: A combination of structural, functional, and mutagenic experiments has been used to study the roles of the invariant Phe82 and highly conserved Leu85 residues in cytochrome *c*, especially with respect to the complexation interface with electron transfer partners and maintenance of the hydrophobic heme pocket. Structural analyses show that the F82Y, L85A, and F82Y/L85A mutant proteins all retain the characteristic cytochrome *c* fold, but that conformational alterations are introduced in the direct vicinity of the mutation sites. In particular, the additional hydroxyl group of Tyr82 is in direct spatial conflict with the side chain of Leu85 in the F82Y mutant protein, leading to rotation of the side chain of Tyr82 out toward the protein surface. This strain is relieved in the F82Y/L85A mutant protein where the phenyl ring of Tyr82 is accommodated in a conformation comparable to that of the phenylalanine normally present at this location. In addition, the available space vacated by the replacement of Leu85 with an alanine allows for the inclusion of two new internal water molecules, one of which is bound to Tyr82 and the other to Arg13. In contrast, in the L85A mutant protein, no internal water molecules are observed in this exclusively hydrophobic pocket, which is partially filled by shifts in nearby side chains. Overall, the conformational changes observed result from the optimization of side chain packing to reflect the spatial requirements of new side chains, the minimization of both vacant internal space and the solvent exposure of hydrophobic groups, and the attainment of maximal hydrogen bonding between available polar groups. It is also clear that the placement of the side chain of Arg13 is dependent on the presence of both Phe82 and Leu85, and one role of these residues may be to restrict the interactions of this side chain to the interactive face of cytochrome *c*. The importance of the integrity of the interactive surface of cytochrome *c* in complexes with electron transfer partners is highlighted by the structural perturbations of this area caused by Tyr82 and other replacements at this position.

Cytochrome *c* provides an ideal focus to address questions concerning those factors that influence the formation of biological electron transfer complexes and the rates at which the associated electron transfer events proceed. Indeed, the nature of such complexes has been the subject of intense scrutiny using a wide range of approaches, varying from theoretical modeling (Poulos & Kraut, 1980; Lum et al., 1987; Tegoni et al., 1993; Guillemette et al., 1994) and computational methods (Wendoloski et al., 1987; Northrup et al., 1988; Northrup et al., 1993) to elucidation of the structure of the complex of yeast iso-1 cytochrome *c* with one of its physiological redox partners, yeast cytochrome *c* peroxidase (Pelletier & Kraut, 1992). This latter complex has also been the focus of numerous functional studies to examine the process of electron transfer once a productive complex has been formed (Erman et al., 1991; Everest et al., 1991; Nocek et al., 1991; Beratan et al., 1992; Corin et al., 1993).

Phe82 is an invariant residue (Hampsey et al., 1988; Moore & Pettigrew, 1990) located in a surface region of cytochrome *c* that forms complexation interactions with electron transfer partners (Louie & Brayer, 1990). Previous structural studies have also shown that Phe82 is an integral component in the maintenance of the hydrophobic heme pocket of cytochrome *c* (Louie et al., 1988b; Louie & Brayer, 1989). Replacement of the side chain of this residue with alternative amino acids has a profound effect on the overall rate of electron transfer activity observed (Pielak et al., 1985; Hilgen & Pielak, 1991; Inglis et al., 1991). Also implicated in being near the site of complex formation with electron transfer partners is the adjacent Leu85 (Burch et al., 1990; Nocek et al., 1991). This residue, like Phe82, plays a dual structural role, being a part of the outer protein surface as well as forming a portion of the internal heme pocket (Louie et al., 1988a).

To gain a better understanding of the function of Phe82 and Leu85 in cytochrome *c*, we have examined the properties of the complementary F82Y, L85A, and F82Y/L85A mutant proteins. These proteins were designed specifically to alter not only the complexation surface of cytochrome *c* but also the nature of the protein medium in this region of the heme pocket.

[†] These studies were supported by grants from the Medical Research Council of Canada to G.D.B. and M.S. T.P.L. and G.V.L. are recipients of MRC Studentships. M.S. is a Career Investigator of the Medical Research Council of Canada.

[‡] Atomic coordinates for the structures discussed herein have been deposited with the Brookhaven Protein Data Bank as entries 1CHH (F82Y), 1CHI (F82Y/L85A), and 1CHJ (L85A).

* Author to whom correspondence should be addressed.

[||] Present address: Department de Microbiologie, Universite de Sherbrooke, Sherbrooke, Quebec, Canada J1H 5N4.

[§] Present address: Structural Biology Laboratory, The Salk Institute, La Jolla, CA 92037.

[⊗] Abstract published in *Advance ACS Abstracts,* November 15, 1994.

0006-2960/95/0434-163$09.00/0

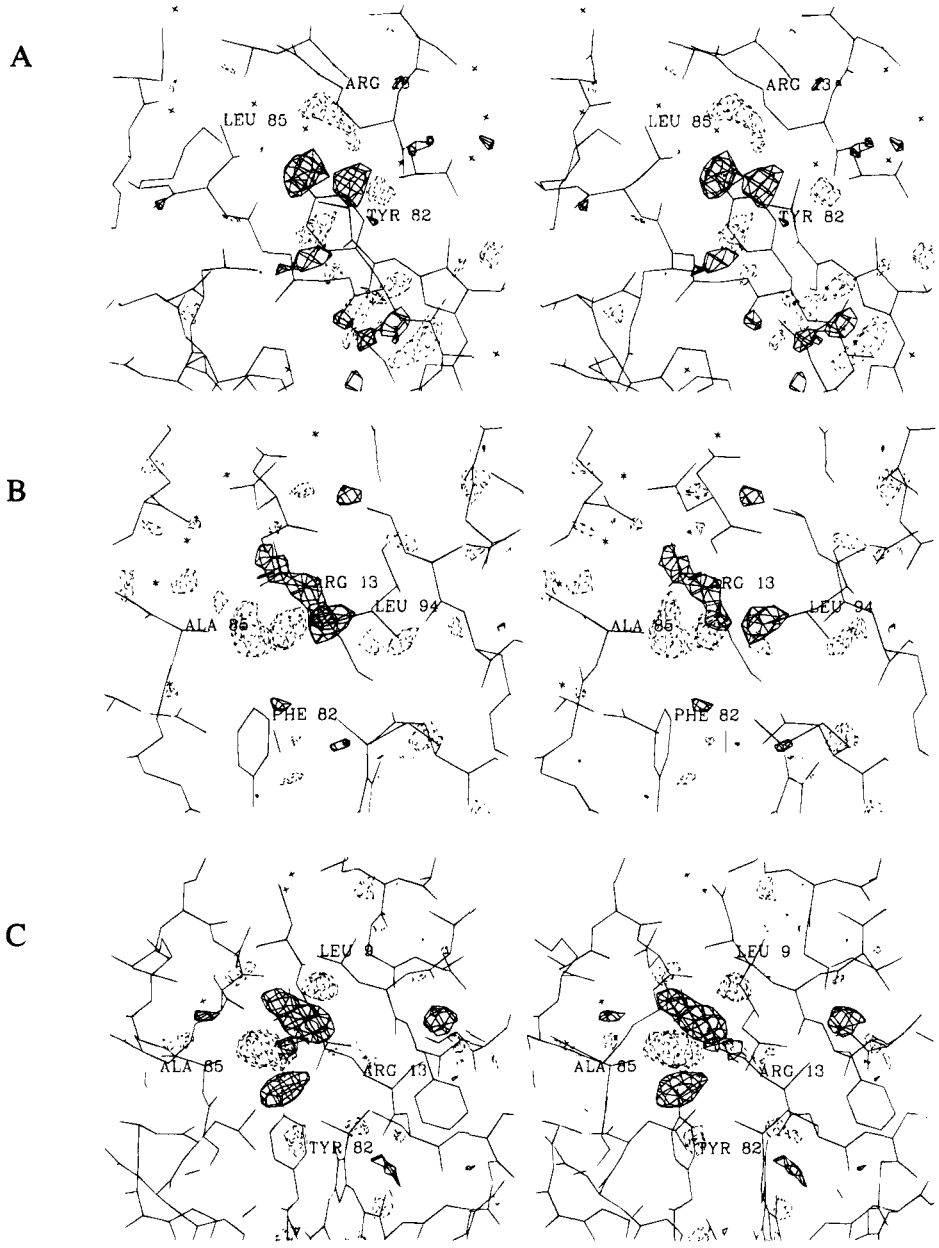

FIGURE 1: Difference electron density maps drawn in the immediate vicinity of mutated residues in (A) F82Y, (B) L85A, and (C) F82Y/L85A yeast iso-1 cytochromes *c*. These maps were calculated using coefficients $F_{mutant} - F_{wild\ type}$, with positive electron density shown as solid contours and negative electron density shown as dashed contours. Overlaid are the final refined mutant protein structures obtained. Water molecule positions are shown as small crosses. Difference electron density for the addition of the Tyr82 hydroxyl group, the loss of the Leu85 side chain, and movement in the side chain of Arg13 is readily apparent.

EXPERIMENTAL PROCEDURES

Mutagenesis and Protein Expression. Mutagenesis of wild-type yeast iso-1 cytochrome *c* was performed as described by Guillemette et al. (1994). In order to avoid covalent homodimer formation, the three mutant iso-1 cytochromes *c* studied were produced with a threonine at residue 102 instead of the naturally occurring cysteine. It has been shown that this substitution is both structurally and functionally neutral (Cutler et al., 1987; Berghuis & Brayer, 1992). The F82Y, L85A, and F82Y/L85A mutants of yeast iso-1 cytochrome *c* were expressed in yeast and purified as described by Rafferty et al. (1990).

X-ray Diffraction Analyses. Crystals of all three mutants of yeast iso-1 cytochrome *c* were grown under reducing conditions similar to those used to grow diffraction quality crystals of the wild-type protein (Sherwood & Brayer, 1985; Louie et al., 1988a). Hanging drop vapor diffusion was employed with either seeding from macrocrystals or hair-seeding from microcrystals (Leung et al., 1989). Crystals of the mutant proteins grew isomorphously to those of wild-type yeast iso-1 cytochrome *c* and are of the space group $P4_32_12$. Unit cell dimensions are summarized in Table 1.

Each mutant cytochrome *c* data set was collected from a single crystal on an Enraf Nonius CAD4-F11 diffractometer having a crystal to counter distance of 36.8 cm and equipped with a helium-filled beam tunnel. A nickel-filtered copper-target X-ray tube with a focal spot of 0.75 × 0.15 mm and operated at 26 mA and 40 kV was used to generate the incident radiation. The ambient temperature was maintained at 15 °C during data collection. The intensity data sets were corrected for backgrounds, absorption (North et al., 1968), crystal decay, and Lorentz and polarization effects as

Table 1: Data Collection and Refinement Parameters

parameter	iso-1 cytochrome *c* mutant F82Y	L85A	F82Y/L85A
cell dimensions (Å)			
$a = b$	36.43	36.60	36.52
c	136.67	138.30	136.74
no. of reflections collected	7073	8140	6823
resolution range for refinement (Å)	6.0−1.97	6.0−1.9	6.0−2.0
data cutoff	$2\sigma(F)$	$2.5\sigma(F)$	$2\sigma(F)$
no. of reflections used in refinement	4546	4886	3761
no. of protein atoms	895	891	892
no. of solvent atoms	70	79	72
average thermal factors (Å^2)			
protein atoms	14.8	15.4	16.6
solvent atoms	23.4	27.2	27.4
R-factor[a]	0.186	0.196	0.185

[a] *R*-factor = $\Sigma|F_o - F_c|/\Sigma|F_o|$.

previously described (Louie et al., 1988a). In order to statistically improve high-resolution intensity measurements for the three diffraction data sets, local background averaging was employed (Louie & Brayer, 1990; Murphy et al., 1992).

Structural refinement was carried out using a restrained parameter least-squares approach (Hendrickson, 1985). Starting models for the three mutant protein structure refinements were based on the wild-type reduced iso-1 cytochrome *c* structure determined to 1.2 Å resolution (Louie & Brayer, 1990). Initial difference electron density maps are shown in Figure 1 for each mutant structure. Examination of these maps allowed alterations to be made in the starting models that reflected the introduction of the mutant residues. All ordered waters with refined isotropic thermal factors under 50 Å^2 from the high-resolution wild-type structure were used in the starting models, except for those that were in close proximity to the mutation sites. These water molecules and those subsequently identified over the course of refinement were modeled as neutral oxygen atoms with full occupancies. The sulfate anion bound to the amino terminal end of the α-helix comprising residues 3−12 in the wild-type structure was also included in the starting models.

At various points during the structure refinements, a sequential examination of the polypeptide chain using omit, $F_o - F_c$, and $2F_o - F_c$ difference electron density maps was conducted to check the progress of refinement and to make manual corrections where necessary. These manual corrections included the identification of additional solvent waters by searching for strong difference electron density peaks within 3.5 Å of hydrogen bond donor or acceptor atoms and the deletion of weakly resolved water molecules. Final refinement parameters for the structures of all three mutant proteins are tabulated in Table 1. All structures exhibit good stereochemistry, and these data are summarized in Table 2.

Atomic coordinate errors for mutant protein structures have been estimated using two methods. Inspection of the Luzzati (1952) plot drawn in Figure 2 indicates that these errors are in the range of 0.18−0.22 Å. Overall atomic coordinate errors can also be estimated by evaluating the individual atomic errors (Cruickshank, 1949, 1954). On the basis of this method, the estimated overall rms coordinate error is 0.16 Å for the F82Y structure, 0.18 Å for the L85A structure, and 0.20 Å for the F82Y/L85A structure.

Direct Electrochemistry. The midpoint reduction potentials of the L85A and F82Y/L85A mutant proteins were obtained by cyclic voltammetry as described by Rafferty et al. (1990). Measurements were taken at a temperature of 25 °C, pH 6.0, and ionic strength $\mu = 0.1$ M.

Table 2: Stereochemical Parameters for Refined Mutant Protein Structures

stereochemical parameter	rms deviation from ideal values F82Y	L85A	F82Y/L85A	restraint weight
distances (Å)				
bond (1−2)	0.019	0.019	0.019	0.020
angle (1−3)	0.038	0.039	0.039	0.030
planar (1−4)	0.045	0.046	0.045	0.045
planes (Å)	0.013	0.012	0.013	0.018
chiral volumes (Å^3)	0.163	0.138	0.159	0.120
nonbonded contacts (Å)[a]				
single torsion	0.212	0.216	0.226	0.250
multiple torsion	0.192	0.220	0.207	0.250
possible hydrogen bonds	0.215	0.239	0.234	0.250
torsion angles (deg)				
planar (0° and 180°)	2.0	1.9	2.0	2.5
staggered (±60°, 180°)	24.7	23.1	23.6	20.0
orthonormal (±90°)	21.7	19.5	17.4	15.0

[a] The rms deviations from ideality for this class of restraint incorporate a reduction of 0.2 Å from the radius of each atom involved in a contact.

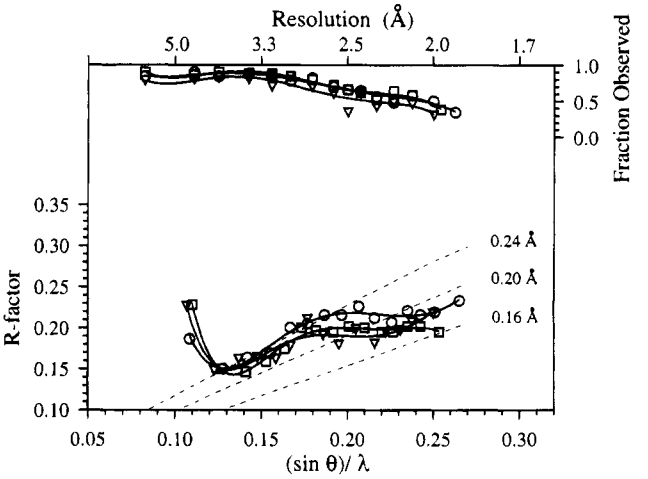

FIGURE 2: Plot of crystallographic *R*-factor as a function of resolution at the end of refinement for the F82Y (□), L85A (○), and F82Y/L85A (▽) mutant cytochromes *c*. The theoretical dependencies of *R*-factor on resolution, assuming various levels of rms error in the atomic positions of the model (Luzzati, 1952), are shown as broken lines. The fraction of theoretical data used in structural refinement is presented on the axis at top right.

Table 3: Overall Average Positional Deviations (Å) between Mutant and Wild-Type Yeast Iso-1 Cytochromes *c*

atom group	iso-1 cytochrome *c* mutant F82Y	L85A	F82Y/L85A
all common protein atoms	0.31	0.37	0.35
all main chain atoms	0.18	0.21	0.22
all common side chain atoms	0.47	0.57	0.52
all heme atoms	0.13	0.15	0.15

RESULTS

As is evident in Figure 3 and Table 3, the overall polypeptide chain folds of the F82Y, L85A, and F82Y/L85A mutant proteins are very similar to that of wild-type iso-1

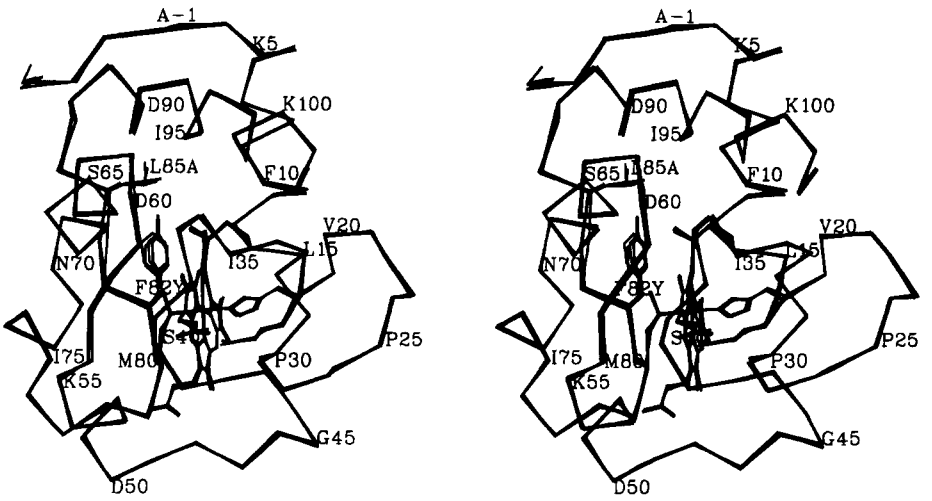

FIGURE 3: Stereo drawing of the α-carbon backbones of the wild-type, F82Y, L85A, and F82Y/L85A iso-1 cytochrome *c* structures. Also drawn are the side chains of the mutated residues, Phe82 and Leu85, and the heme moieties of all four proteins, along with the ligands to the heme iron atom (His18 and Met80) and cysteines 14 and 17, which form covalent thioether bonds to the heme porphyrin ring. Every fifth amino acid residue is indicated by its one-letter amino acid designation and sequence number.

cytochrome *c*. Plots of the average positional deviations of residues along the polypeptide chain of the mutant proteins are shown in Figure 4. The N-terminal residues, Thr(−5) and Glu(−4), are substantially disordered (Louie & Brayer, 1990), and therefore the large positional deviations seen at these positions are the result of positional mobility rather than a reflection of the induced mutations. Tables 4 and 5 show that the overall geometry and solvent exposure of the heme group of each mutant protein are similar to those of wild-type cytochrome *c*. Despite these global similarities, changes in side chain conformations at or near the sites of mutation have occurred in all three structures, and these are discussed in the following sections.

Structure of F82Y Cytochrome c. In wild-type yeast iso-1 cytochrome *c*, the side chain of Leu85 lies directly adjacent to the distal edge of the aromatic ring of the side chain of Phe82. Thus, mutation of Phe82 to a tyrosine places the additional hydroxyl group into direct spatial conflict with the Leu85 side chain. This potential conflict is resolved by the side chain of Tyr82 undergoing a significant positional displacement ($\Delta d = 0.7$ Å), involving a rotation toward the surface of the protein ($\Delta\chi_1 = 3°$, $\Delta\chi_2 = 10°$; Figure 5A). At this location, the side chain of Tyr82 exhibits significantly increased thermal mobility (Table 6), and the hydroxyl group of this residue hydrogen bonds to a surface water molecule. Also having increased thermal mobilities are the main chain atoms of residues 81 and 82. In contrast, the Leu85 side chain retains a position comparable to that in the wild-type structure, with an average deviation of 0.3 Å for side chain atoms. Tyr82 displacement also decreases the angle between the normal of its planar group and that of the heme to 9° from the 23° observed in the wild-type protein. The difference in these values, 14°, is significantly larger than the 4° and 5° observed in the L85A and F82Y/L85A structures, respectively.

Leu9 and Arg13 are two residues in the region of the mutation site that adopt altered conformations. The average side chain deviations observed are 1.1 and 2.5 Å, respectively (Figure 5A). The shift of the side chain of Tyr82 to a more solvent-exposed position necessitates the displacement of the nearby side chain of Arg13. The new conformation of Arg13, as well as the positional shift of Tyr82 toward the protein surface (Figure 5A), accounts for the marked increase in the solvent exposure of the aromatic ring of Tyr82 (Table 7). In contrast, the altered position of the side chain of Arg13 completely masks the side chain of Leu85 from solvent exposure (Table 7). A spatial consequence of Arg13 movement is the displacement of the side chain of Leu9.

Table 4: Heme Geometry of Mutant and Wild-Type Iso-1 Cytochromes *c*[a]

	wild-type	F82Y	L85A	F82Y/L85A
1. Angular Deviations (deg) between the Pyrrole Nitrogen Plane Normal and the Four Individual Pyrrole Ring Plane Normals and the Heme Coordinate Bonds				
A	9.4	9.0	9.2	13.5
B	11.1	11.2	8.8	11.6
C	8.8	8.5	9.2	10.1
D	8.1	9.5	10.2	10.2
Fe−His18 NE2	2.2	2.8	3.3	8.3
Fe−Met80 SD	4.9	2.1	4.3	5.6
2. Angular Deviations (deg) between the Porphyrin Ring Plane Normal and the Four Pyrrole Ring Plane Normals, the Pyrrole Nitrogen Plane Normal, and the Heme Coordinate Bonds				
A	6.7	5.9	5.7	7.9
B	11.9	10.7	10.1	12.4
C	9.8	10.8	9.8	10.5
D	6.0	7.0	6.7	4.7
NNNN	2.6	3.1	3.4	5.6
Fe−His18 NE2	3.2	4.7	0.3	2.9
Fe−Met80 SD	7.5	4.9	7.9	11.1
3. Bond Distances (Å) between the Heme Iron Atom and Its Six Ligands				
His18 NE2	1.98	1.95	1.92	2.14
Met80 SD	2.36	2.28	2.38	2.33
heme NA	1.97	1.98	1.99	2.01
heme NB	2.00	2.02	1.98	2.00
heme NC	1.99	2.02	1.98	2.02
heme ND	2.01	2.05	2.11	2.01

[a] The pyrrole nitrogen plane is defined by the four pyrrole nitrogens of the heme group. The four pyrrole ring planes are each defined by the five atoms of the ring and the first carbon atom attached to each of the four carbons of the ring. The porphyrin ring is defined by the five atoms in each of the four pyrrole rings, the four bridging methine carbon atoms, the first carbon atom at each of the eight side chains of the heme, and the central iron atom of the heme. The heme atom nomenclature used in this table follows the conventions of the Protein Data Bank [see Figure 3 of Berghuis and Brayer (1992)].

Table 5: Heme Solvent Accessibility in Mutant and Wild-Type Yeast Iso-1 Cytochromes *c*[a]

	yeast iso-1 cytochrome *c* structure			
	wild-type	F82Y	L85A	F82Y/L85A
solvent accessible heme atoms and surface area exposed (Å^2)				
CHD	2.9	2.9	2.8	3.1
CMC	9.2	11.2	12.3	9.2
CAC	3.4	4.1	3.3	4.4
CBC	20.1	20.6	18.4	18.3
CMD	10.8	11.2	10.3	10.1
total heme exposure (Å^2)	46.4	50.0	47.1	45.1
total heme surface (Å^2)	513.1	515.0	514.7	512.2
% heme surface area exposed	9.0	9.7	9.2	8.8

[a] Solvent exposure was determined by the method of Connolly (1983) with a probe sphere having a 1.4 Å radius.

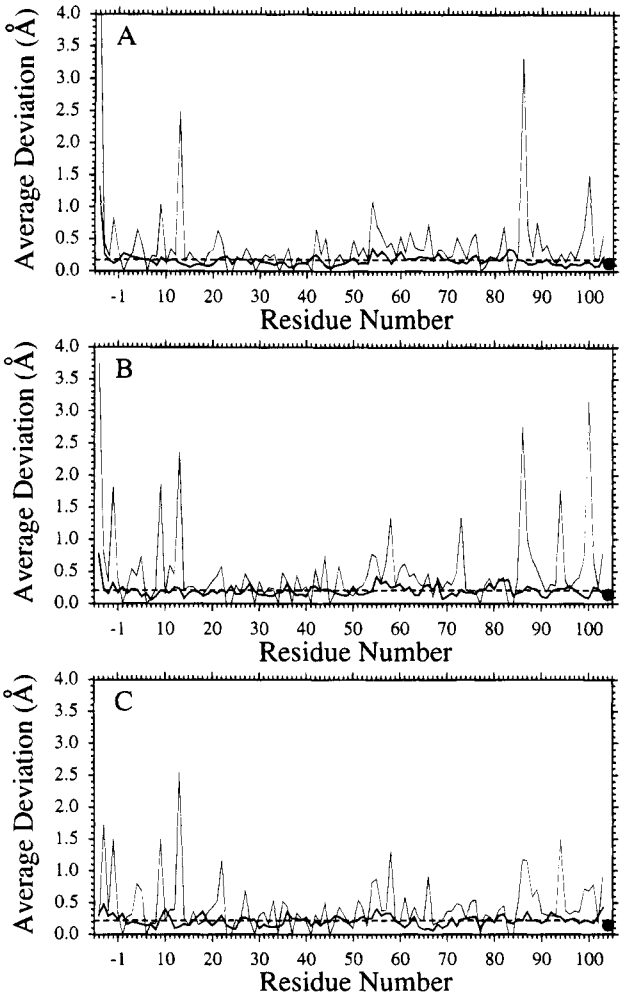

FIGURE 4: Plots of average positional deviations from the wild-type iso-1 cytochrome *c* structure for the (A) F82Y, (B) L85A, and (C) F82Y/L85A mutant proteins. Thick lines indicate average deviations of main chain atoms, while thin lines indicate average deviations of the equivalent side chain atoms. In each diagram, the filled circle at residue position 104 represents the average positional deviation of the heme group, and the horizontal dashed line represents the average positional deviation for all main chain atoms.

The conformation observed for Leu9 ($\chi_1 = -104°$, $\chi_2 = 128°$) in the F82Y protein corresponds well to an alternative conformation observed for this side chain in the high-resolution wild-type structure ($\chi_1 = -111°$, $\chi_2 = 123°$; Louie & Brayer, 1990). In wild-type yeast iso-1 cytochrome *c*, this alternative site appears to have an occupancy of ~30%. Other prominent features in Figure 4A involving side chain groups represent amino acids in the disordered amino terminal region of the polypeptide chain or polar side chains extending from the protein into solvent (Lys54, Lys86, and Lys100).

Table 6: Average Thermal Factors (Å^2) of Residues 80−85[a]

	yeast iso-1 cytochrome *c* structure			
atom groups	wild-type	F82Y	L85A	F82Y/L85A
Met80 main chain	9.9	9.5	10.7	7.4
Met80 side chain	5.2	5.5	8.0	6.2
Ala81	12.0	16.7	11.5	10.7
Phe/Tyr82 main chain	15.2	20.4	13.6	12.1
Phe/Tyr82 side chain	16.9	25.2	10.9	13.2
Gly83	19.0	21.2	16.4	12.4
Gly84	17.4	21.2	17.2	14.3
Leu/Ala85 main chain	13.8	16.3	12.8	13.6
Leu/Ala85 side chain	17.9	12.6	12.9	8.9
all heme atoms	5.3	6.0	7.9	7.6

[a] The average thermal factor for all protein atoms of the wild-type iso-1 cytochrome *c* structure was 16.5 Å^2. The distributions of the protein atomic thermal factors for the three mutants were normalized to this value.

Table 7: Solvent Accessibility of Residues 82 and 85[a]

	yeast iso-1 cytochrome *c* structure			
	wild-type	F82Y	L85A	F82Y/L85A[b]
side chain surface area exposure (Å^2)				
Phe/Tyr82 CD2	10.9	11.8	8.6	10.3
Phe/Tyr82 CE2	6.8	14.2	11.4	12.9
Tyr82 OH		6.9		5.7
Leu85 CD2	13.3	8.7		
total Phe/Tyr82 aromatic ring exposure (Å^2)				
atoms CD2 and CE2	17.7	26.0	20.0	23.2

[a] Solvent-exposed areas were calculated by the method of Connolly (1983), with a probe sphere of 1.4 Å radius. [b] The internal water molecules 224 and 248 were considered to be an integral part of the protein for this calculation.

Structure of L85A Cytochrome c. Mutation of leucine 85 to a much smaller alanine residue creates considerable free volume in this region. In response, the nearby side chains of Leu9, Arg13, and Leu94 have all adopted new conformations (Figures 4B and 5B). The side chain of Leu94 is found to shift ($\Delta d = 1.8$ Å) into the additional space available near Ala85. The side chain of Arg13 also moves toward Ala85 ($\Delta d = 2.4$ Å), and at this new location it forms an interaction with the side chain of Asp90 (Arg13 NH1−Asp90 OD1, $d = 3.6$ Å). This new interaction has a marked effect on the thermal factors of the atoms of the Arg13 side chain, which have an average B of 32.4 Å^2 in the wild-type structure and 16.7 Å^2 in the L85A protein. The movements of both Leu94 and Arg13 appear to cause a shift in the side chain of Leu9 away from the mutation site ($\Delta d = 1.9$ Å) in order to avoid spatial conflicts with these residues. The new conformation of Leu9 differs from both of those seen in the wild-type protein (Louie & Brayer, 1990).

Structure of F82Y/L85A Cytochrome c. In the F82Y/L85A mutant protein, the removal of the side chain of Leu85 allows

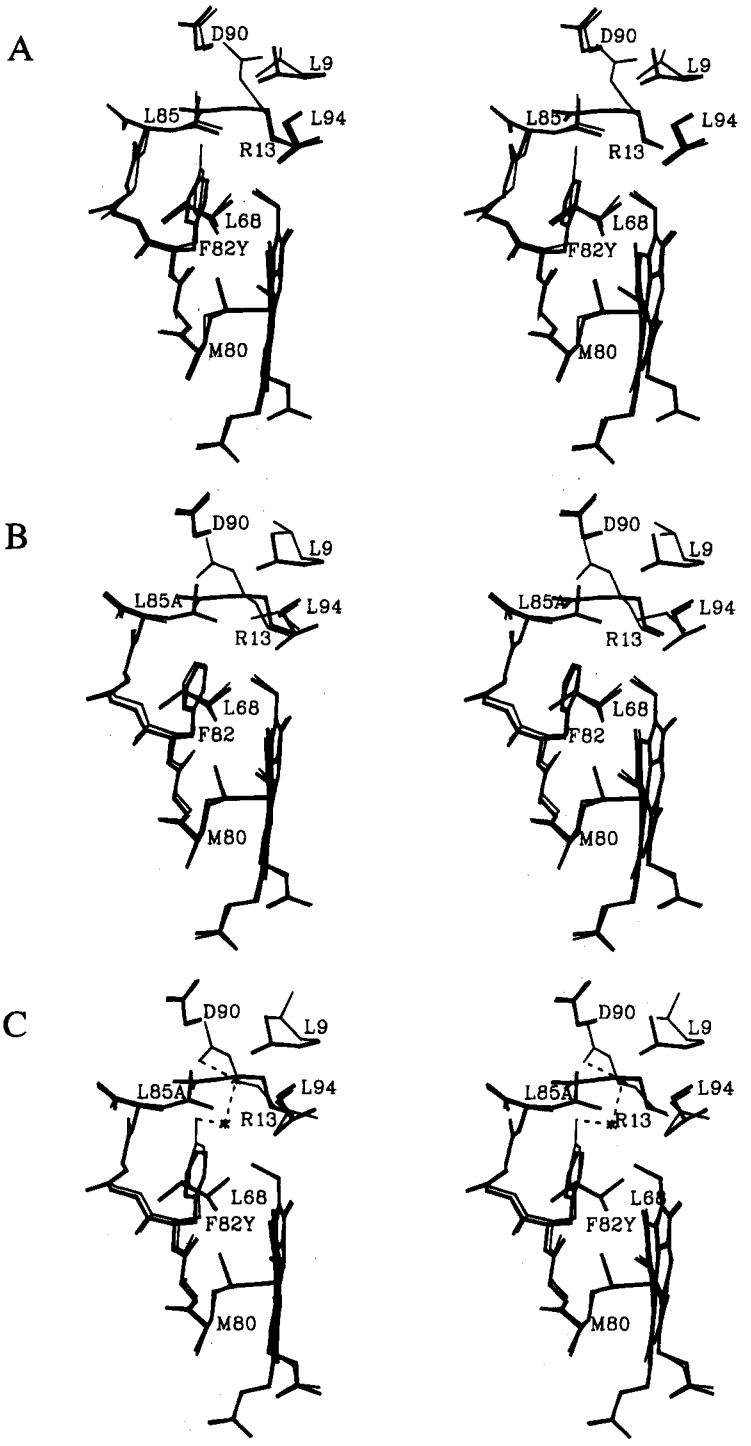

FIGURE 5: Stereodiagrams showing the region about mutated residues in the (A) F82Y, (B) L85A, and (C) F82Y/L85A proteins. In each diagram, the wild-type protein structure has been superimposed and is shown with thick lines, while the mutant protein structures are depicted by thin lines. Altered side chain conformations for Leu9, Arg13, and Leu94 are clearly evident. Two internally bound water molecules (Wat224 and Wat248) observed in the F82Y/L85A mutant protein are depicted as asterisks.

the additional hydroxyl group of Tyr82 to be accommodated with minimal perturbation of the overall position of the phenyl ring of this residue ($\Delta d = 0.4$ Å). As can be seen in Figure 5C, the hydroxyl group of Tyr82 is pointed directly into the region formerly occupied by the Leu85 side chain in the wild-type protein. In addition, two new water molecules are bound in this region, one of which (Wat248) forms a hydrogen bond to the hydroxyl group of Tyr82. The second water molecule (Wat224) hydrogen bonds to the guanidinium group of Arg13, as well as to Wat248 (Figure 5C).

As observed for the L85A protein, the side chain of Arg13 in the F82Y/L85A double mutant moves toward the region vacated by the Leu85 side chain ($\Delta d = 2.6$ Å) and forms a new interaction with the side chain of Asp90 (Arg13 NH1—Asp90 OD1, $d = 3.3$ Å). The average thermal factor for Arg13 side chain atoms is 19.3 Å^2, and as in the L85A mutant protein, this is considerably lower than that found in the wild-type protein. New conformations are also assumed by both Leu9 ($\Delta d = 1.5$ Å) and Leu94 ($\Delta d = 1.5$ Å). As seen in Figure 5C, the Leu9 side chain has shifted away from the mutation site to avoid spatial conflicts with the reposi-

Table 8: Summary of Positional Differences Observed between Mutant and Wild-Type Iso-1 Cytochromes *c*

F82Y	L85A	F82Y/L85A
1. Tyr82 side chain shifts toward surface of protein and its hydroxyl group interacts with a surface water molecule	1. Leu94 side chain moves toward Ala85	1. Leu9 and Leu94 side chains adopt new conformations
2. Tyr82 ring rotates 14° relative to heme plane	2. Leu9 and Arg13 side chains adopt new conformations	2. Arg13 and Asp90 side chains form a new interaction
3. Leu9 and Arg13 side chains adopt new conformations	3. Arg13 and Asp90 side chains form a new interaction	3. Two water molecules are introduced into the mutation site
		4. Tyr82 retains original Phe82 position, with its hydroxyl group interacting with a newly introduced internal water molecule

tioned side chain of Arg13. Unlike the Leu94 shift observed in the L85A mutant protein in the F82Y/L85A double mutant, reorientation of this residue is more localized due to the two newly bound internal water molecules in this region.

DISCUSSION

Structural Consequences of Residue 82 and 85 Mutations. Significant structural changes seen in the F82Y, L85A, and F82Y/L85A mutants of yeast iso-1 cytochrome *c* are summarized in Table 8. These are confined to the region about the mutation sites and reflect an optimization of side chain packing in these proteins, thereby satisfying the spatial requirements of new side chains, the minimization of unoccupied internal space, and the solvent exposure of hydrophobic groups, as well as attaining the maximal hydrogen bonding between available polar groups.

In the F82Y protein, increased spatial requirements are predominant and lead to the rotation of the side chain of Tyr82 toward the protein surface, where its hydroxyl group hydrogen bonds to a surface water molecule. The increased thermal mobility of this residue side chain is indicative of less than optimal side chain packing, which undoubtedly leads to the observed decrease in the stability of this mutant protein (Greene et al., 1993). The induced structural incompatibility found in the F82Y mutant protein is relieved in the F82Y/L85A mutant, which opens up additional space next to the Tyr82 side chain so that it can retain a conformation comparable to that of the normally resident Phe82. The additional space available also allows the hydrogen-bonding potential of the hydroxyl group of Tyr82 to be satisfied by permitting the binding of two new internal water molecules. In the L85A mutant protein, the hydrophobic cavity that otherwise would be created is filled by the side chain of Leu94 and the nonpolar portion of the side chain of Arg13. No internal water molecules are found in this highly hydrophobic interior region, and the positioning of the aromatic group of Phe82 is not affected.

It is clear from these studies that the conformation of Arg13 is dependent on the presence of both Phe82 and Leu85 in the structure of wild-type yeast iso-1 cytochrome *c*. One role of the side chains of Phe82 and Leu85 may be to restrict the potential interaction of Arg13 and Asp90 in order for the former residue to be fully available at the interactive face of cytochrome *c* with redox partners (Pelletier & Kraut, 1992; Northrup et al., 1993; Guillemette et al., 1994). Shifts in the side chain of Arg13 have also been observed in other mutant proteins with replacements at Phe82 (Louie et al., 1988b; Louie & Brayer, 1989).

Table 9: Reduction Potentials for Mutant and Wild-Type Yeast Iso-1 Cytochromes *c*[a]

cytochrome *c*	E_m (mV)
wild-type[b]	290 ± 2
F82Y[b]	280 ± 2
L85A[c]	285 ± 3
F82Y/L85A[c]	283 ± 3

[a] Experimental conditions were: 25 °C, pH 6.0, and μ = 0.1 M. Values are listed relative to a standard hydrogen electrode reference. [b] From Rafferty et al. (1990). [c] From Guillemette et al. (1994).

Impact of Mutations on Reduction Potential. The dielectric constant of the heme pocket is a primary determinant in setting the reduction potential of cytochrome *c* (Kassner, 1973; Louie & Brayer, 1989; Moore & Pettigrew, 1990). Two essential factors affecting the heme pocket dielectric constant are the solvent exposure of the heme moiety and the polarity of amino acids in close proximity to this group. One important structural element in this regard is the side chain of Phe82. For example, the mutation of this residue to serine leads to the creation of a solvent channel into the heme pocket (Louie et al., 1988b), thereby dramatically increasing heme solvent exposure and decreasing the observed reduction potential of this mutant protein (ΔE_m = −35 mV; Rafferty et al., 1990). Similarly, the introduction of polar groups into the heme pocket, occurring as the result of polypeptide rearrangements in the F82G mutant protein (Louie & Brayer, 1989), has a pronounced effect on reduction potential (ΔE_m = −43 mV). By examining a wide range of side chain replacements for Phe82, it is possible to determine that this residue's contribution to the observed +290 mV reduction potential of wild-type yeast iso-1 cytochrome *c* is ca. +40 mV (Rafferty et al., 1990).

Replacement of Phe82 by a tyrosine has a modest impact on heme reduction potential (ΔE_m = −10 mV; Table 9). The increased polarity of the tyrosyl side chain might be expected to have a larger effect, but apparently this is offset by a small positional shift in this group, so that the tyrosyl hydroxyl group is oriented out toward the protein surface where it can interact with solvent molecules (Table 7). In this conformation, the Tyr82 hydroxyl group is quite distant (d = 6.5 Å) from the porphyrin ring of the heme and is shielded from direct heme plane contact by the CBB side chain atom of the heme group. In addition, the hydrophobicity of the heme pocket remains intact since the tyrosyl ring remains in position to shield the heme from any significant increase in solvent exposure (Table 5).

In both the L85A and F82Y/L85A mutant cytochromes *c*, even smaller effects are seen on heme reduction potential (Table 9). For the L85A mutant protein, this is to be expected since the side chain of Phe82 retains its wild-type

conformation and the internal cavity left by the replacement of Leu85 is filled by the hydrophobic portions of other side chains (Figure 5). Thus, the hydrophobic integrity of the heme pocket is preserved in this mutant protein, and the reduction potential is not significantly perturbed.

Although the hydroxyl group of Tyr82 takes on a more internal positioning and two new water molecules are bound in the F82Y/L85A mutant (Figure 5, Table 7), this has only a small effect on heme reduction potential (Table 9). This result is somewhat surprising given the larger impacts of the glycine and serine substitutions at Phe82 (Louie et al., 1988b; Louie & Brayer, 1989). However, this might be explained by the fact that the tyrosyl hydroxyl and the two newly bound internal water molecules, which contribute to increased polarity in the mutation site, are substantially further removed from the heme plane than are the polar groups introduced in the F82S and F82G mutant proteins. In these latter proteins, the newly introduced polar groups not only are located immediately adjacent to the central face of the heme plane but are also near the central heme iron atom. In the F82Y/L85A protein, the tyrosyl hydroxyl group is projected away from the heme porphyrin ring (d = 6.5 Å), and the new internal water molecules are located along the heme edge where heme substituent side chains shield direct access to the porphyrin ring. The shortest heme porphyrin ring plane to water distance is 5.4 Å. Thus, it appears that the increased local polarity introduced into the F82Y/L85A mutant protein is too distant from the central heme porphyrin core to substantially affect heme reduction potential.

Electron Transfer in Mutant Proteins. The steady-state rate of the electron transfer reaction of yeast iso-1 cytochrome *c* with yeast cytochrome *c* peroxidase varies considerably upon the mutation of Phe82, with the F82Y, F82S, and F82G proteins having 30%, 70%, and 20% of wild-type activity, respectively (Pielak et al., 1985). Similar trends were observed for the activity of these mutants in the electron transfer reaction with bovine cytochrome *c* oxidase (Michel et al., 1989). Such decreases in the reaction rate may arise from perturbation of either the intrinsic rate of electron transfer within these protein−protein complexes or the interactions that are a part of the formation of such complexes. Recent studies have shown that the multiphasic kinetics observed in the electron transfer reaction between reduced iso-1 cytochrome *c* and a Zn-substituted cytochrome *c* peroxidase porphyrin π cation radical does not require the presence of an aromatic residue at position 82 of cytochrome *c* (Everest et al., 1991). Studies of electron transfer between bovine cytochrome *c* oxidase and iso-1 cytochromes *c* with the replacement of Phe82 produced similar conclusions (Hazzard et al., 1992).

The fact that the kinetics of intracomplex electron transfer involving Phe82 mutants of iso-1 cytochrome *c* does not correspond to the steady-state activity decreases observed for these proteins suggests that complex formation with redox partners is the major factor influencing these changes in steady-state activity. This is supported by the proposed interactive surface of cytochrome *c*, as elucidated by modeling of such complexes (Poulos & Kraut, 1980; Lum et al., 1987; Northrup et al., 1988), and the recent determination of the structure of the complex formed between yeast iso-1 cytochrome *c* and cytochrome *c* peroxidase (Pelletier & Kraut, 1992). In this latter complex, Phe82 is completely sequestered within the region of protein−protein interactions, although the side chain of Arg13 and several water molecules prevent Phe82 from making direct contact with the cytochrome *c* peroxidase molecule. In the case of the F82Y mutant protein, the side chain of Tyr82 would protrude from the surface of the protein into the site of complexation and, in conjunction with corresponding movements of the Arg13 side chain, would disrupt the formation of a productive electron transfer complex. This could explain the considerably lower steady-state activity of this mutant protein. In contrast, the mutation of Phe82 to serine does not present such a physical intrusion into the interaction region of the complex, and steady-state activity is affected to a lesser extent. The lower rate of the Ser82 protein could be attributed to the increase of solvent molecules in this region, leading to somewhat less specific complex surface interactions. Another example of a large change in the contour of the complex contact surface can be found in the mutation of Phe82 to glycine in which the exposed face of cytochrome *c* is drastically altered. As would be expected from the present work, this greatly reduces the steady-state electron transfer rate.

Thus, there appears to be a close relationship between the integrity of the complexation surface of cytochrome *c* and the overall electron transfer activity observed. The importance of this factor is further emphasized by the observed species specificity in attaining optimal protein−protein electron transfer reactions involving cytochrome *c* (Ho et al., 1985; Nocek et al., 1991; Moench et al., 1992, 1993). Such effects on electron transfer most likely arise from differences in the makeup of the interactive surface of cytochrome *c* between species, not unlike the structural changes that have been introduced by site-directed mutagenesis.

ACKNOWLEDGMENT

The authors thank Michael Murphy, Albert Berghuis, and Stephen Evans for insightful discussions and computational expertise, as well as Connie Leung and Theresa Yang for technical assistance. Prof. Grant Mauk provided facilities for the electrochemistry experiments.

REFERENCES

Beratan, D. N., Onuchic, J. N., Winkler, J. R., & Gray, H. B. (1992) *Science 258*, 1740−1741.

Berghuis, A. M., & Brayer, G. D. (1992) *J. Mol. Biol. 223*, 959−976.

Burch, A. M., Rigby, S. E. J., Funk, W. D., MacGillivray, R. T. A., Mauk, M. R., Mauk, A. G., & Moore, G. R. (1990) *Science 247*, 831−833.

Connolly, M. L. (1983) *Science 221*, 709−713.

Corin, A. F., Hake, R. A., McLendon, G., Hazzard, J. T., & Tollin, G. (1993) *Biochemistry 32*, 2756−2762.

Cruickshank, D. W. J. (1949) *Acta Crystallogr. 2*, 65−82.

Cruickshank, D. W. J. (1954) *Acta Crystallogr. 7*, 519.

Cutler, R. L., Pielak, G. J., Mauk, A. G., & Smith, M. (1987) *Protein Eng. 1*, 95−99.

Erman, J. E., Kang, D. S., Kim, K. L., Summers, F. E., Matthis, A. L., & Vitello, L. B. (1991) *Mol. Cryst. Liq. Cryst. 194*, 253−258.

Everest, A. M., Wallin, S. A., Stemp, E. D. A., Nocek, J. M., Mauk, A. G., & Hoffman, B. M. (1991) *J. Am. Chem. Soc. 113*, 4337−4338.

Greene, R. M., Betz, S. F., Hilgen-Willis, S., Auld, D. S., Fencl, J. B., & Pielak, G. J. (1993) *J. Inorg. Biochem. 51*, 663–676.

Guillemette, J. G., Barker, P. D., Eltis, L. D., Lo, T. P., Smith, M., Brayer, G. D., & Mauk, A. G. (1994) *Biochemie 76*, 592–604.

Hampsey, D. M., Das, G., & Sherman, F. (1988) *FEBS Lett. 231*, 275–283.

Hazzard, J. T., Mauk, A. G., & Tollin, G. (1992) *Arch. Biochem. Biophys. 298*, 91–95.

Hendrickson, W. A. (1985) *Methods Enzymol. 115*, 252–270.

Hilgen, S. E., & Pielak, G. J. (1991) *Protein Eng. 4*, 575–578.

Ho, P. S., Sutoris, C., Liang, N., Margoliash, E., & Hoffman, B. M. (1985) *J. Am. Chem. Soc. 107*, 1070–1071.

Inglis, S. C., Guillemette, J. G., Johnson, J. A., & Smith, M. (1991) *Protein Eng. 4*, 569–574.

Kassner, R. J. (1973) *J. Am. Chem. Soc. 95*, 2674–2677.

Leung, C. J., Nall, B. T., & Brayer, G. D. (1989) *J. Mol. Biol. 206*, 783–785.

Louie, G. V., & Brayer, G. D. (1989) *J. Mol. Biol. 210*, 313–322.

Louie, G. V., & Brayer, G. D. (1990) *J. Mol. Biol. 214*, 527–555.

Louie, G. V., Hutcheon, W. L. B., & Brayer, G. D. (1988a) *J. Mol. Biol. 199*, 295–314.

Louie, G. V., Pielak, G. J., Smith, M., & Brayer, G. D. (1988b) *Biochemistry 27*, 7870–7876.

Lum, V. R., Brayer, G. D., Louie, G. V., Smith, M., & Mauk, A. G. (1987) *Protein Struct., Folding Des. 2*, 143–150.

Luzzati, V. (1952) *Acta Crystallogr. 5*, 802–810.

Michel, B., Mauk, A. G., & Bosshard, H. R. (1989) *FEBS Lett. 243*, 149–152.

Moench, S. J., Chroni, S., Lou, B.-S., Erman, J. E., & Satterlee, J. D. (1992) *Biochemistry 31*, 3661–3670.

Moench, S. J., Erman, J. E., & Satterlee, J. D. (1993) *Int. J. Biochem. 25*, 1335–1342.

Moore, G. R., & Pettigrew, G. W. (1990) *Cytochromes c: Evolutionary, Structural and Physicochemical Aspects*, Springer-Verlag, Berlin.

Murphy, M. E. P., Nall, B. T., & Brayer, G. D. (1992) *J. Mol. Biol. 227*, 160–176.

Nocek, J. M., Stemp, E. D. A., Finnegan, M. G., Koshy, T. I., Johnson, M. K., Margoliash, E., Mauk, A. G., Smith, M., & Hoffman, B. M. (1991) *J. Am. Chem. Soc. 113*, 6822–6831.

North, A. C. T., Phillips, D. C., & Mathews, F. S. (1968) *Acta Crystallogr., Sect. A 24*, 351–359.

Northrup, S. H., Boles, J. O., & Reynolds, J. C. L. (1988) *Science 241*, 67–70.

Northrup, S. H., Thomasson, K. A., Miller, C. M., Barker, P. D., Eltis, L. D., Guillemette, J. G., Inglis, S. C., & Mauk, A. G. (1993) *Biochemistry 32*, 6613–6623.

Pelletier, H., & Kraut, J. (1992) *Science 258*, 1748–1755.

Pielak, G. J., Mauk, A. G., & Smith, M. (1985) *Nature (London) 313*, 152–154.

Poulos, T. L., & Kraut, J. (1980) *J. Biol. Chem. 255*, 10322–10330.

Rafferty, S. P., Pearce, L. L., Barker, P. D., Guillemette, J. G., Kay, C. M., Smith, M., & Mauk, A. G. (1990) *Biochemistry 29*, 9365–9369.

Sherwood, C., & Brayer, G. D. (1985) *J. Mol. Biol. 185*, 209–210.

Tegoni, M., White, S. A., Roussel, A., Mathews, F. S., & Cambillau, C. (1993) *Proteins: Struct., Funct., Genet. 16*, 408–422.

Wendoloski, J. J., Matthew, J. B., Weber, P. C., & Salemme, F. R. (1987) *Science 238*, 794–796.